Synthesis, self-assembly and photovoltaic applications of tribenzopentaphene derivatives†

Ching-En Chou,[a] Yong Li,[a] Yanke Che,[b] Ling Zang[b] and Zhonghua Peng*[a]

Four tribenzopentaphene (TBP) derivatives containing different alkoxy side chains have been synthesized and shown to self-assemble into different microobjects such as microspheres, microfibers and microribbons. Photovoltaic cells of **1b** blended with PDI or $PC_{61}BM$ are fabricated and preliminary results show good efficiencies comparable to those of previously reported photovoltaic devices of hexabenzocoronenes.

Introduction

Discotic polycyclic aromatic hydrocarbons (PAHs) have been attracting great attention from structural, environmental, and more recently molecular electronics perspectives.[1–13] Their often planar or near-planar geometry and extended π-delocalization render them appealing π–π stacking building blocks which can be utilized to dictate controlled self-assembly processes. In addition, the potentially high charge mobility along the stacked PAH column may find applications in sensors, field effect transistors and photovoltaic cells.[14–21] While a number of PAHs such as triphenylenes, hexabenzocoronenes, *etc.* have been extensively studied as molecular electronic materials, derivatives with a tribenzopentaphene (TBP) core have drawn less attention.[22,23] A notable exception is a recent publication on alkyl-substituted TBP derivatives.[24] We have been working on alkoxy-substituted TBPs and TBP-containing conjugated foldamers. In this contribution, we report the synthesis and characterizations of four new TBP derivatives whose structures are shown in Chart 1. Their optical, electrochemical, self-assembly, and photovoltaic properties are discussed.

Results and discussion

Synthesis

As shown in Chart 1, all four compounds have two dodecyloxy chains at the bay positions which make them soluble in common organic solvents, even when there is no other substituent (compound **1a**). Compounds **1b** and **1c** bear four methoxy and

isopropoxy groups, respectively, while compound **1d** has four hydroxyl groups around the periphery. These TBP derivatives were synthesized according to Scheme 1. The key steps are the Suzuki–Miyaura coupling of biarylboronic acid derivatives (**4a**, **4b**, **4c**) with 1,2-bis(dodecyloxy)-4,5-diiodobenzene to form *o*-quinquephenyls (**5a**, **5b**, **5c**)[25–28] and the subsequent Scholl oxidative cyclization to yield the TBP core.[29,30] The Suzuki–Miyaura coupling went smoothly and could proceed directly from 2-bromobiaryl derivatives (**3a**, **3b**, **3c**) as a one-pot synthesis with good overall yields (around 50%).[31] The Scholl reactions of alkoxy-substituted oligophenylenes are often complicated as previously shown by other researchers.[32,33] Competing side reactions such as incomplete cyclization, electrophilic aromatic halogenation, inter-molecular oxidative coupling, *etc.* often lead to a messy reaction mixture from which the pure desired product is difficult to isolate. After experimenting with different oxidants ($MoCl_5$,[34] $FeCl_3$, and DDQ[35]), solvent combinations, oxidant/substrate ratios, and temperatures, the best results were obtained by using 5–10 equivalents of $FeCl_3$ in a nitromethane–dichloromethane solvent mixture at 0 °C. Under these conditions, compounds **1a**, **1b** and **1c** were obtained in 15–30% yields.
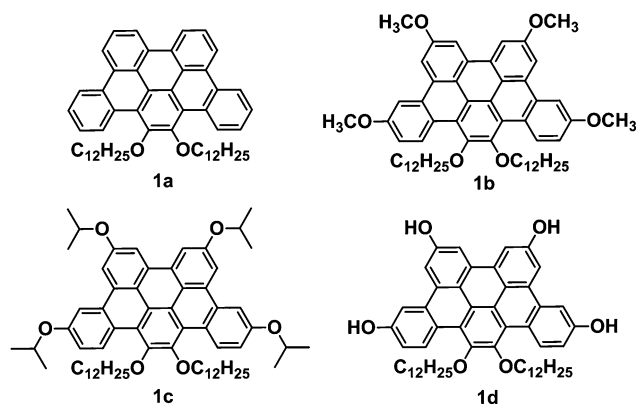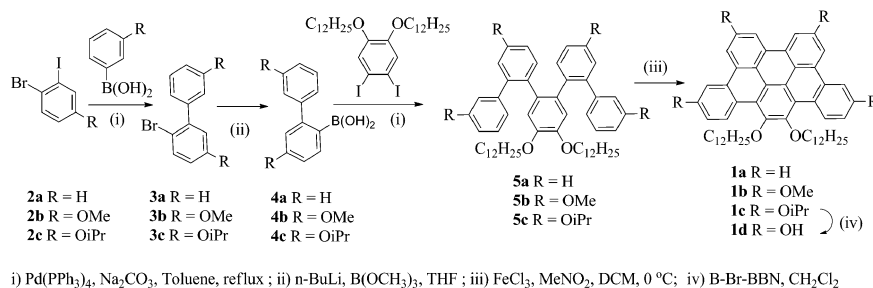
[a]Department of Chemistry, University of Missouri-Kansas City, Kansas City, Missouri, 64110, USA. E-mail: PengZ@umkc.edu

[b]Department of Materials Science and Engineering, University of Utah, Salt Lake City, Utah 84108, USA

† Electronic supplementary information (ESI) available: ^{1}H and ^{13}C NMR spectra of **1a–1d**; 2D COSY ^{1}H NMR spectra of **1a–1d**; DSC thermograms of **1a–1c**; POM images of **1a–1c** during cooling from melt; SEM images of self-assembled objects of **1a–1d**; solar cell configuration. See DOI: 10.1039/c3ra43392g

Chart 1 Structures of four tribenzopentaphene derivatives.

Scheme 1 Synthesis of TBP derivatives.

i) Pd(PPh₃)₄, Na₂CO₃, Toluene, reflux ; ii) n-BuLi, B(OCH₃)₃, THF ; iii) FeCl₃, MeNO₂, DCM, 0 °C; iv) B-Br-BBN, CH₂Cl₂

Compound **1d** was synthesized from **1c** in excellent yield using B-bromo-9-BBN as the dealkylation reagent.

Compounds **1a**, **1b** and **1c** are soluble in common organic solvents such as chloroform, dichloromethane, and THF, while compound **1d** is soluble in acetone and THF. Their structures and purity have been confirmed by ^{1}H & ^{13}C NMR, MALDI-TOF MS measurements, and elemental analysis. Fig. 1 shows the ^{1}H NMR spectra of the aromatic region of the four TBP compounds, where sharp and well resolved signals are observed. The assignment of all signals was made based on the chemical shifts, multiplicity, integrations and confirmed by their 2D COSY spectra (see the ESI† for 1D and 2D NMR spectra of all four compounds). Compounds **1b** and **1c** show five aromatic signals: two doublets and three singlets (or two dd and three d under high resolution) while compound **1d** shows two additional singlets in the aromatic region which can be assigned to the two types of hydroxyl protons. It is noted that the two adjacent aromatic protons "a" and "e" in all four compounds (labeled as "a" and "g" in compound **1a**) have very different chemical shifts, differing by more than 2.5 ppm. The unusually high chemical shift of protons "a" is likely due to H-bonding with the oxygen atom in the adjacent bay area alkoxy group.

Optical properties

Fig. 2 shows the UV-Vis absorption spectra of the four TBPs in chloroform and as solid films. In solution, all four compounds
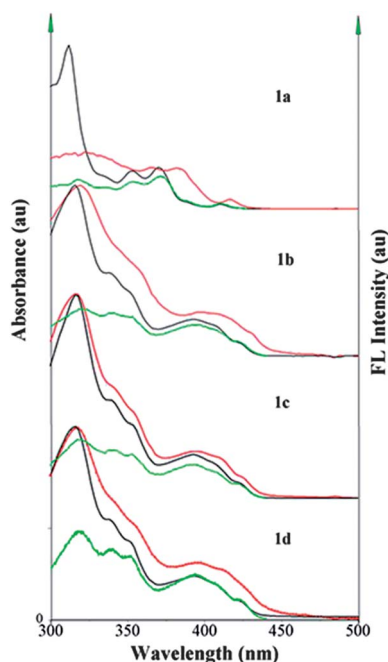

Fig. 2 UV-Vis absorption (black) and excitation (green) spectra of the four TBP compounds in chloroform solutions. The red curves are the absorption spectra of the TBP films.
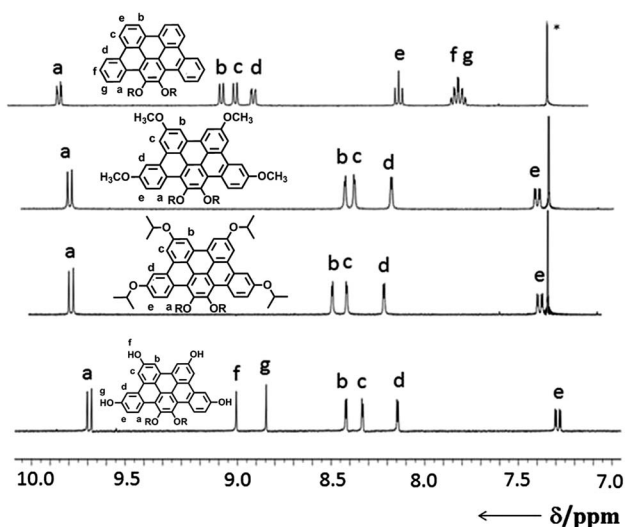
showed a strong band at around 315 nm and a number of less intense bands at longer wavelengths. For **1a** with only two alkoxy substituents at the bay positions, two moderately strong bands at 354 nm and 370 nm and one much weaker band at 410 nm are observed. The 410 nm, 354/370 nm, and 312 nm bands are α, p, and β bands, respectively, following Clar's classification.[36] The energy ratio of the β band over the α band is 1.314, slightly deviated from the 1.35 ratio normally observed for uniplanar PAHs, indicating the twisting of some rings which results in the loss of some resonance energy.[37] It is noted that the three prominent bands (β and p bands) of **1a** (312, 354 and 370 nm bands) closely match those of its alkyl analog (two alkyl groups instead of two alkoxy groups at the bay positions).[24] The α band of **1a** is however bathochromically shifted by 15 nm, compared to that of its alkyl analog.[24] When four additional alkoxy (or hydroxyl in the case of **1d**) groups are attached to the outskirt of the TBP core, significant bathochromic shift (~40 nm) of the p band is observed which is now partially overlapped with the weaker α band as shown in the absorption spectra of

Fig. 1 ^{1}H NMR spectra (aromatic region) of the four TBP compounds.

1b, **1c** and **1d** in Fig. 2. The α band is also red-shifted but with a much less amount (∼12 nm) while the β band shows negligible shift. When the absorption spectra of films are compared to those of solutions, one notices a 8 nm red-shift in band-edge for **1a**, **1b** and **1d** but only 3 nm red-shift in **1c**, indicating much weaker inter-TBP π–π stacking interactions due to the steric blocking effect of those bulky isopropoxy groups.

All four TBPs show moderate fluorescence (FL) in solutions. Fig. 3 shows the emission spectra of both solutions and films of the four TBPs. The solution FL emission spectra of **1b**, **1c** and **1d** are nearly identical with a maximum emission wavelength λ_{max} of 432 nm, while the emission λ_{max} of **1a** is 418 nm. The fluorescence quantum yields of **1a**, **1b**, **1c** and **1d** in chloroform are 0.16, 0.27, 0.30, and 0.17, respectively (370 nm excitation for **1a** and 394 nm excitation for the other three compounds). The TBP films are also fluorescent. While the films of **1a**, **1b** and **1d** all gave a red-shifted, broad, and featureless emission band, the emission of film **1c** shows two bands closely matching its solution emission spectrum, again indicating the much weaker π–π stacking interaction in **1c** than in **1a**, **1b** and **1d**. When the excitation spectra are compared to the absorption spectra (Fig. 2), one sees close matching of the two spectra in the α and p bands region for all four compounds. The β band in the excitation spectra is however much weaker than that in the absorption spectra, indicating inefficient energy transfer from the excited β band to the emissive S$_1$ state.

Electrochemistry

Cyclic voltammetry (CV) measurements were carried out in oxygen-free dichloromethane solutions for all compounds
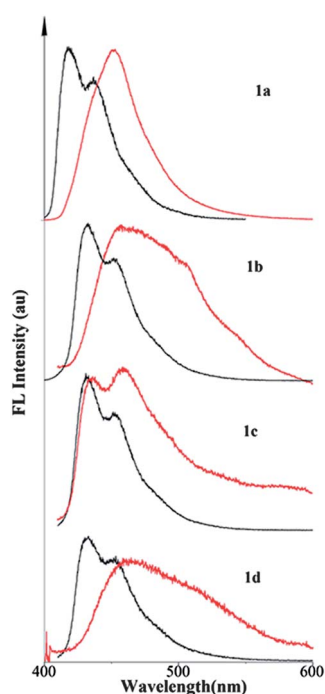
except for **1d** which was measured in an acetone solution. As shown in Fig. 4, TBPs **1a**, **1b** and **1c** all show a reversible oxidation wave with half-cell potentials of 0.87, 0.55, and 0.42 V, respectively, while **1d** shows a semi-reversible oxidation wave with an oxidation peak potential (E_{pa}) of 0.78 V and an estimated half-cell potential of 0.73 V. Under identical conditions, a reversible oxidation wave ($E_{1/2} = 0.15$ V) is observed for the ferrocene/ferrocenium couple. Using the ferrocene energy level of 4.8 eV below vacuum, the HOMO energy levels of **1a**, **1b**, **1c**, and **1d** were calculated to be −5.67, −5.35, −5.21 eV, and −5.38 eV, respectively. The gradual increase in HOMO energy levels from **1a** to **1d** to **1b** to **1c** reflects the increasing electron-donating effect of the alkoxy substituents. No reduction wave was observed for all four compounds within the scan range of 0 to −2 V.

Self-assembly

When methanol or hexane vapor was diffused into the chloroform solutions of **1a**, **1b**, **1c**, and THF solution of **1d**, the clear solutions became opaque in a day or two. The opaque solutions were drop-casted onto silicon wafer, vacuum dried and then sputter-coated with an ultrathin layer of gold. Field-emission scanning electron microscope (SEM) XL30 (FEI Company, Hillsboro, OR) was used with an accelerating voltage of 5.0 kV. The SEM images (Fig. 5) of the **1a** and **1b** films show fiber structures which are tens to even hundreds of microns long and have a fairly uniform diameter of ∼200 nm. The fiber structures of **1a** appear to be flexible as they are coiled, bended, and entangled together, while the fiber structures of **1b** seem more rigid as they are mostly straight and oriented along the same direction.

Compound **1d**, on the other hand, aggregates to give microspheres with an average diameter of ∼500 nm. Compound **1c** yields no well-defined aggregated structures. The different self-assembled structures of the four TBP compounds reflect clearly the effect of the different ring substituents. With small peripheral groups (Hs for **1a** and MeO for **1b**), strong π–π stacking interactions are expected which drive the formation of
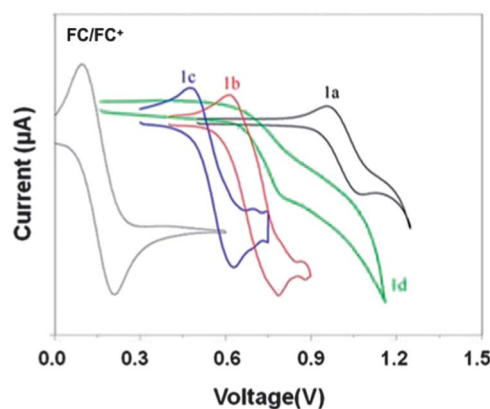

Fig. 3 Fluorescence emission spectra of the four TBP compounds in chloroform solutions (black) and as solid films (red).

Fig. 4 Cyclic voltammograms of **1a**, **1b**, and **1c** in CH$_2$Cl$_2$ and **1d** in acetone solutions (the voltammogram of **1d** was corrected based on Fc/Fc$^+$ internal standard in acetone).
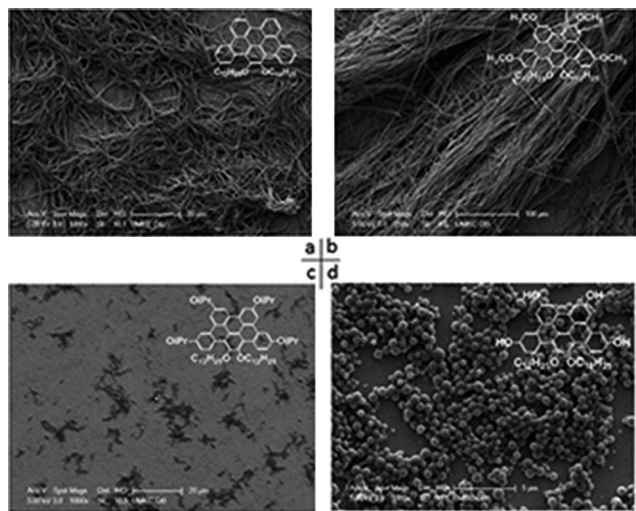
Fig. 5   SEM images of self-assembled structures of **1a** (a), **1b** (b), **1c** (c) and **1d** (d). Scale bars: 20 μm for **1a**, 100 μm for **1b**, 20 μm for **1c**, 5 μm for **1d**.

long fiber structures.[38] Compound **1d** has four hydroxyl substituents. In addition to π–π stacking interactions perpendicular to the TBP ring, there may exist strong H-bonding in lateral directions. Furthermore, the amphiphilicity of compound **1d** may dictate the self-assembled structures as well. The overall result is the formation of microspheres. With four bulky isopropoxy groups, compound **1c** lacks strong π–π stacking interactions, which significantly slows its self-assembly process. Such results are consistent with the optical property studies.

Photovoltaic properties

The lack of reduction process, the high HOMO energy level and the well-defined one dimensional fiber-shaped self-assembly prompted us to explore further the applications of **1b** as photoinduced electron donors in a non-covalently bonded donor–acceptor (D–A) system for solar cells. Specifically, bulk heterojunction solar cells using **1b** as the electron donor and *N*,*N*′-di(dodecyl)-perylene-3,4,9,10-tetracarboxylic diimide (PDI) or [6,6]-phenyl-C$_{61}$ butyric acid methyl ester (PC$_{61}$BM) as the electron acceptor were fabricated with a device structure of indium tin oxide (ITO)/PEDOT:PSS/**1b** : PDI (or PC$_{61}$BM)/Ca/Al. Fig. 6 shows the absorption spectra of the mixtures of **1b** : PDI and **1b** : PC$_{61}$BM (1 : 1, wt ratio) in chloroform and thin film, respectively. The spectra of the mixtures in solution are a simple
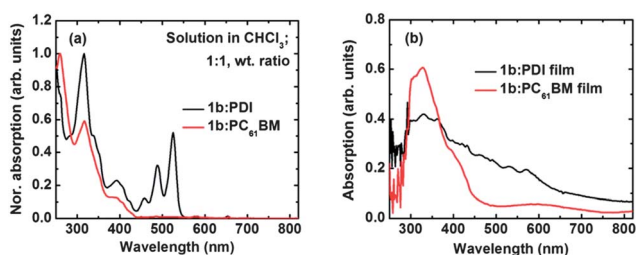

Fig. 6   UV-Vis absorption spectra of **1b** : PDI and **1b** : PC$_{61}$BM (1 : 1, wt ratio) in chloroform (a) and as annealed thin films (b).
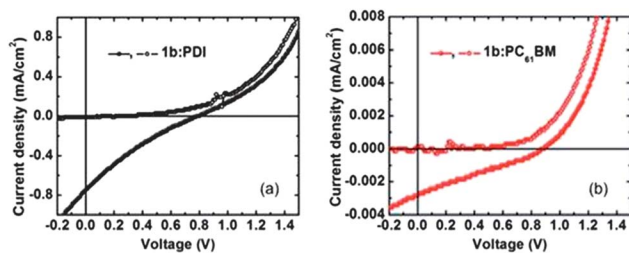

Fig. 7   *J–V* curves of the solar cells fabricated from **1b** : PDI (a) and **1b** : PC$_{61}$BM (b) in dark and under illumination.

linear superimposition of the individual components. As for the blend film of **1b** : PDI, a significantly broadened absorption with a long tail extending to over 800 nm was observed as compared to its absorption spectrum in solution. This indicates a strong aggregation in the **1b** : PDI film. Both homostacking of **1b** and/or PDI, and heterostacking between **1b** and PDI (donor–acceptor stacking) may occur simultaneously and contribute to the spectral broadening and bathochromic shift. On the other hand, the film spectrum of **1b** : PC$_{61}$BM showed broadened peaks only at wavelengths below 450 nm which is corresponding to the **1b** homo-π–π stacking. A weak but discernible broad peak from 500 to 700 nm was contributed by PC$_{61}$BM aggregation.[39]

Fig. 7 shows the current density–voltage (*J–V*) characteristics of the solar cells. The blend film of **1b** : PDI exhibited an efficiency of 0.12% with a V_{OC} of 0.78 V, a J_{SC} of 0.75 mA cm^{-2}, and a FF of 0.21. This efficiency is comparable to those of previously reported photovoltaic devices of hexabenzocoronene:PDI blends.[40] The blend film of **1b** : PC$_{61}$BM showed poor performance with an efficiency of only 6.8×10^{-6} with a V_{OC} of 0.87 V, a J_{SC} of 0.0029 mA cm^{-2}, and a FF of 0.27. This is likely due to the dramatically different molecular shapes of **1b** and PC$_{61}$BM which prevents an intimate blending of the two components/domains. Further optimization of the solar cells is under investigation.

Conclusions

In summary, four alkoxy-substituted TBP derivatives have been synthesized and characterized. All four compounds are moderately fluorescent in dilute solutions when excited at their α or p bands. Excitation at the β band (~315 nm, the strongest absorption band), however, gave much lower fluorescence quantum yields. The TBP rings exhibit strong π–π stacking interactions in **1a**, **1b** and **1d** but not so much in **1c** due to the steric effect of the four bulky isopropoxy groups. Driven by the strong π–π stacking interaction, **1a** and **1b** self-assemble into microfibers. With additional hydrogen bonding and amphiphilic interactions coming into play, compound **1d** aggregates into microspheres. Compound **1c** on the other hand fail to assemble into well-defined structures under similar conditions. Photovoltaic cells using **1b** as the electron donor and PDI or PC$_{61}$BM as the electron acceptor have been fabricated. The **1b** : PDI blend showed better photovoltaic performance and a power conversion efficiency of 0.12% has been obtained.

Experimental section

General remarks

All the reactions were carried out under nitrogen protection. The solvents were used after fresh distillation over drying agents indicated and were transferred under nitrogen: THF (Na–benzophenone), CH_2Cl_2 (CaH_2). $PC_{61}BM$ was purchased from Nano-C, Inc. All the other reagents were purchased from Sigma-Aldrich and were used without further purification. 1-Bromo-2-iodo-4-methoxybenzene (**2b**), and 1-bromo-2-iodo-4-isopropoxybenzene (**2c**) were synthesized according to literature procedures.[41] Compounds **3a–3c** were synthesized by palladium-catalyzed Suzuki coupling reactions of aryl boronic acid and aryl halide of literature method.[25–28] PDI was synthesized following published procedures.[42] The ^{1}H and ^{13}C NMR spectra were recorded on a Varian INOVA 400 MHz FT NMR spectrometer in the solvent indicated; chemical shifts (δ) are given in ppm relative to TMS, coupling constant (J) in Hz. The solvent signals were used as references[43] ($CDCl_3$: δ_C = 77.16 ppm; residual $CHCl_3$ in $CDCl_3$: δ_H = 7.26 ppm; acetone-d6: δ_C = 206.26, 29.84 ppm; residual acetone in acetone-d6: δ_H = 2.05 ppm). UV-Vis absorption spectra were measured using a Hewlett-Packard 8452A diode array spectrophotometer. Emission and excitation spectra were measured using a Shimadzu RF-5301PC spectrofluorophotometer. Fluorescence quantum yield for solution was determined using quinine sulfate in 1 N H_2SO_4 (φ = 0.58) as the standard. CV studies were carried out in freshly distilled dichloromethane for **1a**, **1b**, **1c** and acetone for **1d** under argon protection at room temperature using a BAS Epsilon EC electrochemical station employing a platinum working electrode (MF-2013) of 1.6 mm in diameter, a silver wire as the reference electrode, and a Pt wire as the counter electrode. [Bu$_4$N]PF$_6$ was used as the supporting electrolyte. The scan rate for all the measurements was set at 50 mV s^{-1}. Ferrocene was used as an internal standard. MALDI-TOF measurements were carried out on a Voyager DE Pro (Perspective Biosystem/ABI) mass spectrometer, operating in linear and reflector mode. Dithranol (1,8-dihydroxyanthrone) and a mixture of silver trifluoroacetate–dithranol (1 : 25, w/w) were used as the matrix.

Synthesis

The Suzuki–Miyaura coupling leading to compounds **5a**, **5b**, and **5c**, and their subsequent Scholl reactions to compounds **1a**, **1b**, and **1c** were exemplified by the synthesis of **5a** and **1a**.

Compound 5a. Under nitrogen atmosphere, *n*-BuLi (4.8 mL of 2.5 M solution, 12 mmol) was added dropwise to a solution of 2-bromobiphenyl (**3a**) (2.00 g, 8.58 mmol) in dry THF (35 mL) at −78 °C. The resulting solution was stirred for 1 h, followed by the addition of trimethyl borate (1.78 g, 17.2 mmol). The resulting mixture was stirred at room temperature overnight. To the above solution were added toluene (40 mL), ethanol (40 mL) and water (18 mL), followed by N_2 bubbling for 45 min. 1,2-Bis(dodecyloxy)-4,5-diiodobenzene (2.40 g, 3.43 mmol), sodium carbonate (2.19 g, 20.6 mmol) and Pd(PPh$_3$)$_4$ (0.119 g, 0.103 mmol) were then added. The resulting reaction mixture was

stirred at 90 °C for 48 h under nitrogen atmosphere and was then poured into water. The mixture was extracted with dichloromethane several times. The organic phase was collected and dried over anhydrous magnesium sulfate. After removing the solvent, the liquid residue was purified by column chromatography on silica gel (hexanes/CH_2Cl_2, 2/1, v/v) to afford the product as white crystals (1.26 g, 49%, mp 41–42 °C). ^{1}H NMR (400 MHz, $CDCl_3$): δ 7.05 (br, 12H), 6.86 (br, 2H), 6.70 (br, 2H), 6.63 (br, 2H), 6.15 (br, 2H), 3.90 (br, 4H), 1.79 (br, 4H), 1.27–1.43 (br, 36H), 0.88 (m, 6H); ^{13}C NMR (400 MHz, $CDCl_3$): δ 147.81, 141.60, 140.35, 139.45, 133.03, 131.66, 129.34, 127.74, 127.00, 126.59, 126.03, 116.80, 69.15, 32.09, 29.88, 29.83, 29.80, 29.62, 29.54, 29.37, 26.17, 23.03, 22.86, 14.30, 14.27.

Compound 5b. Yellow oil (44%). ^{1}H NMR (400 MHz, $CDCl_3$): δ 6.94 (br, 2H), 6.67 (br, 6H), 6.44 (br, 2H), 6.30 (br, 2H), 6.22 (br, 2H), 6.11 (br, 2H), 3.93 (br, 4H), 3.79 (s, 6H), 3.60 (s, 6H), 1.80 (br, 4H), 1.43–1.27 (br, 36H), 0.89 (m, 6H); ^{13}C NMR (400 MHz, $CDCl_3$): δ 159.12, 158.09, 147.89, 142.75, 141.08, 133.15, 132.95, 132.81, 132.40, 128.48, 121.67, 116.95, 114.76, 113.44, 112.90, 112.42, 69.38, 55.37, 55.01, 32.09, 29.88, 29.84, 29.81, 29.62, 29.54, 29.42, 26.19, 22.86, 14.30.

Compound 5c. Yellow oil (68%). ^{1}H NMR (400 MHz, $CDCl_3$): δ 6.91 (br, 2H), 6.60 (br, 6H), 6.41 (br, 2H), 6.26 (br, 4H), 6.12 (br, 2H), 4.47 (br, 2H), 4.18 (br, 2H), 3.85 (br, 4H), 1.76 (br, 4H), 1.18–1.42 (br, 60H), 0.88 (m, 6H); ^{13}C NMR (400 MHz, $CDCl_3$): δ 157.36, 156.39, 147.87, 142.88, 141.31, 133.20, 132.79, 132.14, 128.62, 121.63, 117.01, 116.86, 115.90, 114.59, 69.93, 69.66, 69.30, 32.09, 29.88, 29.83, 29.81, 29.60, 29.53, 29.42, 22.85, 22.47, 22.33, 22.25, 21.96, 14.29.

Compound 1a. A solution of anhydrous FeCl$_3$ (0.56 g, 3.45 mmol) in CH_3NO_2 (5.0 mL) was added dropwise to a solution of **5a** (0.26 g, 0.346 mmol) in dry CH_2Cl_2 (20 mL) with nitrogen bubbling through a two-neck round bottom flask at 0 °C. When the addition was completed, the ice bath was removed and resulting solution was stirred at room temperature for another hour. The reaction was quenched with CH_3OH (30 mL) and water (10 mL). The resulting mixture was stirred for 1 h. The organic layer was collected and the aqueous layer was extracted by dichloromethane three times (30 mL each). The combined dichloromethane extracts were dried over anhydrous MgSO$_4$. After filtration, the filtrate was stripped of solvent. The residual yellowish solid was purified by column chromatography (hexanes/CH_2Cl_2, 40/1 to 10/1, v/v), to give **1a** as light yellow solids (52 mg, 20%, mp 101–102 °C). ^{1}H NMR (400 MHz, $CDCl_3$): δ 9.87 (d, J = 8 Hz, 2H), 9.00 (d, J = 8 Hz, 2H), 8.92 (d, J = 8 Hz, 2H), 8.82 (d, J = 8 Hz, 2H), 8.05 (t, J = 8 Hz, 2H), 7.77 (m, 4H), 4.19 (t, J = 8 Hz, 4H), 2.03 (m, 4H), 1.26 (m, 36H), 0.87 (m, 6H); ^{13}C NMR (400 MHz, $CDCl_3$): δ 150.76, 130.81, 130.02, 129.78, 129.57, 129.11, 127.69, 127.23, 126.41, 124.71, 123.44, 122.74, 122.11, 122.02, 121.51, 74.56, 45.17, 32.10, 30.78, 29.89, 29.86, 29.84, 29.83, 29.55, 26.46, 22.87, 14.30. MS (MALDI-TOF): [M + H]$^+$ calcd 744.49, found 744.31; anal calcd for $C_{54}H_{64}O_2$ (744.49): C, 87.05; H, 8.66; found: C, 86.79; H, 8.42.

Compound 1b. Bright yellow solids (30%, mp: 119–120 °C). ^{1}H NMR (400 MHz, $CDCl_3$): δ 9.82 (dd, J = 12 Hz, 2H), 8.35 (d, J = 4 Hz, 2H), 8.30 (d, J = 4 Hz, 2H), 8.10 (d, J = 2 Hz, 2H), 7.33 (dd, J = 12 Hz, 2H), 4.18 (s, 6H), 4.16 (t, J = 8 Hz, 4H), 4.09

(s, 6H), 2.03 (t, $J = 8$ Hz, 4H), 1.25 (m, 36H), 0.88 (m, 6H); ^{13}C NMR (400 MHz, CDCl$_3$): δ 158.67, 157.88, 149.62, 132.03, 131.59, 131.29, 130.91, 124.17, 120.35, 120.33, 115.45, 107.90, 107.68, 106.27, 105.16, 74.35, 55.93, 55.62, 32.10, 30.80, 29.91, 29.89, 29.85, 29.55, 26.50, 22.87, 14.29; MS (MALDI-TOF): [M + H]$^+$ calcd 864.53, found 864.13; anal calcd for C$_{58}$H$_{72}$O$_6$: C, 80.52; H, 8.39; found: C, 80.56; H, 8.29.

Compound 1c. Bright yellow liquid which slowly solidified after a few weeks (15%, mp 54–55 °C). ^{1}H NMR (400 MHz, CDCl$_3$): δ 9.81 (d, $J = 8$ Hz, 2H), 8.41 (s, 2H), 8.34 (s, 2H), 8.13 (s, 2H), 7.32 (d, $J = 12$ Hz, 2H), 5.04 (t, $J = 8$ Hz, 2H), 4.90 (t, $J = 8$ Hz, 2H), 4.17 (t, $J = 8$ Hz, 4H), 2.03 (t, $J = 8$ Hz, 4H), 1.55 (m, 12H), 1.51 (m, 12H), 1.27 (m, 36H), 0.88 (m, 6H); ^{13}C NMR (400 MHz, CDCl$_3$): δ 156.93, 156.14, 149.53, 132.17, 131.58, 131.32, 130.81, 123.97, 121.19, 120.41, 120.29, 116.51, 110.27, 109.72, 108.86, 74.28, 70.78, 70.19, 32.10, 30.81, 29.91, 29.90, 29.86, 29.56, 26.50, 22.87, 22.48, 22.43, 14.30; MS (MALDI-TOF): [M + H]$^+$ calcd 976.66, found 976.16; anal calcd for C$_{66}$H$_{88}$O$_6$: C, 81.1; H, 9.07; found: C, 80.89; H, 8.81.

Compound 1d. B-Bromo-9-BBN (1 M solution of dichloromethane, 0.66 mL, 0.66 mmol) was added dropwise to a dichloromethane solution of compound **1c** (0.15 g, 0.15 mmol in 5 mL of CH$_2$Cl$_2$) under refluxing. The resulting mixture was refluxed at 45 °C overnight. The reaction mixture was washed with 4 N NaOH solution (three times) and then with water. The organic layer was collected and dried over MgSO$_4$. The crude product obtained by solvent evaporation was further purified by recrystallization from methanol–THF to get the targeted compound as brown solids (0.10 g, 85%). ^{1}H NMR (400 MHz, acetone-d6): δ 9.82 (d, $J = 8$ Hz, 2H), 9.04 (s, 2H), 8.88 (s, 2H), 8.45 (s, 2H), 8.37 (s, 2H), 8.18 (s, 2H), 7.32 (d, $J = 12$ Hz, 2H), 4.25 (t, $J = 8$ Hz, 4H), 1.66 (t, $J = 8$ Hz, 4H), 1.20 (m, 42H); ^{13}C NMR (400 MHz, (CD$_3$)$_2$CO): δ 157.84, 157.13, 150.24, 133.19, 132.63, 132.33, 131.82, 123.89, 121.84, 120.97, 120.09, 117.69, 110.38, 109.96, 108.92, 74.84, 32.84, 31.50, 27.28, 23.53, 14.55; MS (MALDI-TOF): [M + H]$^+$ calcd 808.47, found 808.07; anal calcd for C$_{54}$H$_{64}$O$_6$: C, 80.16; H, 7.97; found: C, 79.89; H, 8.32.

Photovoltaic devices fabrication and characterization

ITO coated glass slides with sheet resistance of 8–12 Ω square^{-1} was used as substrates. ITO glass was cut into 1.5 cm by 1.5 cm pieces, and the ITO was patterned by etching with aqua regia vapor. The patterned ITO glass substrates were cleaned in an ultrasonic bath sequentially by detergent, water, deionized water, toluene, acetone, and isopropyl alcohol, each for 15 min, and then dried by compressed air stream. Cleaned ITO substrates were treated with UV ozone for 45 min before use. Highly conductive poly(3,4-ethylenedioxythiophene):poly(styrenesulfonate) (PEDOT:PSS, Clevios P VP AI4083) thin layer was spin-coated (4000 RPM, 30 s) onto the ITO substrates from an aqueous solution. The substrates were dried at 120 °C for 45 min on hotplate in air. Blend solutions of **1b** : PDI (1 : 1 wt ratio; 10 mg mL^{-1}) and **1b** : PC$_{61}$BM (1 : 1 wt ratio; 10 mg mL^{-1}) were prepared in glove box by dissolving respective materials in CHCl$_3$. The solutions were heated at 50 °C with stirring for 48 h and passed through a 0.45 µm filter before spin coating. The active layer was deposited by spin-coating the solution of respective active materials on top of the PEDOT:PSS layer. The devices were transferred to glove box and dried in nitrogen atmosphere under reduced pressure. The films were annealed at 80 °C for 20 h in nitrogen atmosphere. Subsequently, an electrode including 45 nm thick Ca and 100 nm thick Al was deposited on the top by thermal evaporation under high vacuum (<2 × 10^{-6} mb). The active area of 0.14 cm^2 of the devices was defined by the area of deposited Ca/Al electrode through a shadow mask.

Current–voltage characteristics were measured using a Keithley 2400 SourceMeter. Devices were illuminated with an Oriel Xenon Arc Lamp Solar Simulator at an intensity of 100 mW cm^{-2} (1-sun air mass 1.5 global illumination). Short circuit current density (J_{SC}), open circuit voltage (V_{OC}), and maximum output power density ($J_{max}V_{max}$) were obtained from the J–V curves under illumination. The power conversion efficiency was calculated by $\eta = J_{SC}V_{OC}FF/P_{in}$, where P_{in} is the incident power density; and FF is fill factor which is given by $J_{max}V_{max}/J_{SC}V_{OC}$.

Acknowledgements

Notes and references

1 M. D. Watson, A. Fechtenkötter and K. Müllen, *Chem. Rev.*, 2001, **101**, 1267.

2 W. Pisula, M. Kastler, D. Wasserfallen, T. Pakula and K. Müllen, *J. Am. Chem. Soc.*, 2004, **126**, 8074.

3 P. Samori, X. Yin, N. Tchebotareva, Z. Wang, T. Pakula, F. Jackel, M. D. Watson, A. Venturini, K. Müllen and J. P. Rabe, *J. Am. Chem. Soc.*, 2004, **126**, 3567.

4 X. Feng, W. Pisula, L. Zhi, M. Takase and K. Müllen, *Angew. Chem., Int. Ed.*, 2008, **47**, 1703.

5 C. Liu, A. Fechtenkötter, M. D. Watson, K. Müllen and A. Bard, *Chem. Mater.*, 2003, **15**, 124.

6 S. J. Kang, S. Ahn, J. B. Kim, C. Schenck, A. M. Hiszpanski, S. Oh, T. Schiros, Y. L. Loo and C. Nuckolls, *J. Am. Chem. Soc.*, 2013, **135**, 2207.

7 S. Laschat, A. Baro, N. Steinke, F. Giesselmann, C. Haegele, G. Scalia, R. Judele, E. Kapatsina, S. Sauer, A. Schreivogel and M. Tosoni, *Angew. Chem., Int. Ed.*, 2007, **46**, 4832.

8 X. Feng, W. Pisula and K. Müllen, *Pure Appl. Chem.*, 2009, **81**, 2203.

9 H. K. Bisoyi and S. Kumar, *Chem. Soc. Rev.*, 2010, **39**, 264.

10 (a) S. Kumar, *Liq. Cryst.*, 2009, **36**, 607; (b) S. Kumar, W. Pisula and Y. H. Geerts, *Chem. Soc. Rev.*, 2007, **36**, 1902; (c) S. Kumar, *Chem. Soc. Rev.*, 2006, **35**, 83.

11 Y. Li, P. Lu, X. Yan, L. Jin and Z. Peng, *RSC Adv.*, 2013, **3**, 545.

12 (a) C. Chou, D. Wang, J. F. Hsu, Y. Liu and Z. Peng, *Synth. Met.*, 2009, **159**, 1657; (b) C. E. Chou, D. Wang, M. Bagui, J. Hsu, S. Chakraborty and Z. Peng, *J. Lumin.*, 2010, **130**, 986.

13 B. R. Kaafarani, *Chem. Mater.*, 2011, **23**, 378.

14 J. P. Hill, W. Jin, A. Kosaka, T. Fukushima, H. Ichihara, T. Shimomura, K. Ito, T. Hashizume, N. Ishii and T. Aida, *Science*, 2004, **304**, 1481.

15 L. Schmidt-Mende, A. Fechtenkötter, K. Müllen, E. Moons, R. H. Friend and J. D. MacKenzie, *Science*, 2001, **293**, 1119.

16 W. Pisula, A. Menon, M. Stepputat, I. Lieberwirth, U. Kolb, A. Tracz, H. Sirringhaus, T. Pakula and K. Müllen, *Adv. Mater.*, 2005, **17**, 684.

17 S. Xiao, J. Tang, T. Beetz, X. Guo, N. Tremblay, T. Siegrist, Y. Zhu, M. Steigerwald and C. Nuckolls, *J. Am. Chem. Soc.*, 2006, **128**, 10700.

18 (*a*) W. W. H. Wong, C. Ma, W. Pisula, C. Yan, X. Feng, D. V. Jones, K. Müllen, R. A. J. Janssen, P. Bauerle and A. B. Holmes, *Chem. Mater.*, 2010, **22**, 457; (*b*) F. Jackel, M. D. Watson, K. Műllen and J. P. Rabe, *Phys. Rev. Lett.*, 2004, **92**, 188303.

19 Y. Li, Y. Bian, M. Yan, P. S. Thapaliya, D. Johns, X. Yan, D. Galipeau and J. Jiang, *J. Mater. Chem.*, 2011, **21**, 11131.

20 G. Horowitz, *Adv. Mater.*, 1998, **10**, 365.

21 C. J. Brabec, N. S. Sariciftci and J. C. Hummelen, *Adv. Funct. Mater.*, 2001, **11**, 15.

22 Y. Lu and J. S. Moore, *Tetrahedron Lett.*, 2009, **50**, 4071.

23 M. Müller, C. Kübel and K. Müllen, *Chem.–Eur. J.*, 1998, **4**, 2099.

24 B. Alameddine, S. M. Caba, M. Schindler and T. A. Jenny, *Synthesis*, 2012, 1928.

25 N. Miyaura, K. Yamada and A. Suzuki, *Tetrahedron Lett.*, 1979, **20**, 3437.

26 N. Miyaura and A. Suzuki, *Chem. Rev.*, 1979, **95**, 2457.

27 J. F. W. McOmie, M. L. Watts and D. E. West, *Tetrahedron*, 1968, **24**, 2289.

28 H. Lee, J. Oh, H. Y. Chu, J. I. Lee, S. H. Kim, Y. S. Yang, G. H. Kim, L. M. Do, T. Zyung, J. Lee and Y. Park, *Tetrahedron*, 2003, **59**, 2773.

29 N. Boden, R. J. Bushby, A. N. Cammidge, S. Duckworth and G. Headdock, *J. Mater. Chem.*, 1997, **7**, 601.

30 N. Boden, R. J. Bushby, G. Headdock, O. R. Lozman and A. Wood, *Liq. Cryst.*, 2001, **28**, 139.

31 N. G. Andersen, S. P. Maddaford and B. A. Keay, *J. Org. Chem.*, 1996, **61**, 9556.

32 Q. Zang, P. Prins, S. C. Jones, S. Barlow, T. Kondo, Z. An, L. D. Siebbeles and S. R. Marder, *Org. Lett.*, 2005, **7**, 5019.

33 S. H. Wadumethrige and R. Rathore, *Org. Lett.*, 2008, **10**, 5139.

34 B. T. King, J. Kroulík, C. R. Robertson, P. Rempala, C. L. Hilton, J. D. Korinek and L. M. Gortari, *J. Org. Chem.*, 2007, **72**, 2279.

35 L. Zhai, R. Shukla and R. Rathore, *Org. Lett.*, 2009, **11**, 3474.

36 E. Clar, in *Polycyclic Hydrocarbons*, Academic Press, London, UK, 1964, vol. 2.

37 E. Clar and D. G. Stewart, *J. Am. Chem. Soc.*, 1952, **74**, 6235.

38 L. Zang, Y. Che and J. S. Moore, *Acc. Chem. Res.*, 2008, **41**, 1596.

39 P. Boland, S. S. Sunkavalli, S. Chennuri, K. Foe, T. Abdel-Fattah and G. Namkoong, *Thin Sold Films*, 2010, **518**, 1728.

40 H. C. Hesse, J. Weickert, M. Al-Hussein, L. Dössel, X. Feng, K. Müllen and L. Schmidt-Mende, *Sol. Energy Mater. Sol. Cells*, 2010, **94**, 560.

41 A. Fürstner and J. W. J. Kennedy, *Chem.–Eur. J.*, 2006, **12**, 7398.

42 H. Langhals, *Heterocycles*, 1995, **40**, 477.

43 H. E. Gottlieb, V. Kotlyar and A. Nudelman, *J. Org. Chem.*, 1997, **62**, 7512.